Inoculation mechanism of rare earth–Mg alloy in molten cast iron

Q. CHEN*
Materials Research Institute, Sheffield Hallam University, City Campus, Pond Street, Sheffield, S1 1WB, UK

C. WANG
Department of Mechanical Engineering, Tianjin University, Tianjin 300072, Peoples Republic of China

The dissolution region of RE–Mg (RE = rare earth) alloy in the reaction chambers of in-mould inoculated castings was studied by scanning electron microscopy and on electron microprobe. The dissolution region of the inoculant was divided into 7 zones according to its microstructure. The RE–Mg alloy is composed of Mg_2Si, a Mg_2Si–Si eutectic, FeSi, RE–Mg–Si and other silicides. The dissolution of the alloy is a process in which the low melting point phases such as Mg_2Si, a Mg_2Si–Si eutectic and RE–Mg–Si dissolve first, and the high melting point phases such as FeSi and $FeSi_2$ dissolve later. In addition, some intermediate products form during the dissolution process. This causes a concentration gradient of Mg and RE in the melt which results in a transition of the graphite morphology from normal spheroid to open nodule, vermicular and flake graphite. The dissolution of the FeSi phase in the melt forms local sites of high silicon concentration which promote the nucleation and growth of the graphite. © *1998 Chapman & Hall*

1. Introduction

Observation of the dissolution behaviour of the inoculant in a cast iron melt is an important approach to provide an understanding of the mechanism of inoculation and graphite formation in grey cast iron [1, 2]. However since the general treatment of spheroidal cast iron with RE–Mg (RE = rare earth) alloys causes stirring and convection of iron melts no experimental observation of the dissolution behaviour of RE–Mg alloys has been achieved. In the inmold ductile iron process, the dissolution of a spheroidizer takes place in the reaction chamber, which is under a static pressure due to the molten cast iron [3–5]. The spheroidizer sometimes partially melts and preserves the dissolution region of the alloy in the reaction chamber [6]. Therefore it is possible to study the dissolution behaviour of an RE–Mg alloy in the molten iron and its effects on the nucleation and growth of spheroidal graphite.

In this paper the experimental procedure to obtain the dissolution region and to analyse the composition and the microstructure of the dissolution region is presented. The mechanism of the formation of the dissolution region and inoculation and growth of graphite are also discussed.

2. Experimental procedures

The spheroidizer (whose composition is shown in Table I) was introduced into the reaction chamber as a part of the gating system as is shown in Fig. 1. The charge consisted of a low impurity pig iron and was melted in an acid-lined, high-frequency induction furnace. The liquid iron was superheated to 1500 °C and was tapped into a ladle and 1 wt % CaC_2 was added for desulphurizing. Then the melts were immediately poured into the mould with a pouring temperature of 1340 °C. The composition of the melts were as follows: 3.9–4.1 wt % C, 1.9–2.2 wt % Si, 0.6–0.8 wt % Mn, 0.03–0.05 wt % S, balance Fe.

Metallographic specimens were cut from the bottom of the reaction chamber and ground with successively finer grades of silicon carbide paper. They were finally polished using diamond paste lubricated by alcohol in order to reveal the dissolution region of the spheroidizer. In order to observe the 3-dimensional morphology of graphite by scanning electron microscopy (SEM), part of the specimens were deep-etched with 5% methanol bromide.

An Olympus optical microscope was also used to examine the specimens. A scanning electron microscope, Philips SEM 505, was used for the microstructural

---

* Author to whom correspondence should be addressed.

observations. A Philips EDX-9100 energy dispersive spectrometer and a Joel JAX-50A wavelength dispersive spectrometer were used in the elemental distribution analysis of the specimens.

3. Results

The phase constitution of the RE–Mg alloy was determined using an electron microprobe. The phases observed to be present in the sample are labelled on a secondary electron image of a polished section of an RE–Mg alloy sample in Fig. 2. The quantitative analysis data of the corresponding points numbered in Fig. 2 are listed in Table II.

The RE–Mg alloy consists of various phases as shown in Fig. 2 and Table II. Mg, RE and Ca tend to segregate and are hardly dissolved, existing as compounds in the Fe–Si alloy.

The dissolution region consists of structures that are graded from those in the RE–Mg alloy to those in cast iron. The region can be divided into seven zones according to (i) the amount of silicon in the matrix as shown in Table III and (ii) the graphite morphology as shown in Fig. 3.

Zone I is the parent alloy described in Section 1. A detail of zone II is shown in Fig. 4. The matrix of zone II is the ε FeSi phase which contains 50 at % (corresponding to 33 wt %) silicon and the quantitative

measurement results of the corresponding points are listed in Table IV. Comparing the results in Table IV with those of the alloy listed in Table II, it can be seen that there is little difference in the composition of the phases between the two zones with the exception of the amount of Fe. It seems that Fe diffuses into the inoculant alloy, so that the $FeSi_2$ in the alloy changes into FeSi + Si, and the free Si diffuses into the liquid iron. The Mg_2Si–Si eutectic fragments into small pieces. It appears that Mg partially dissolves in the molten cast iron. Both violet grey crystals (silicon carbide) and equiaxial Mg_2Si crystals can be found in this zone using optical microscopy.

Small Mg_2Si and Mg–RE–Si phase particles are dispersed between zones II and III as is shown in Fig. 5 and for which the compositions of the measured points are listed in Table IV. Zone III can be seen in the upper part of Fig. 5 with a matrix consisting of the α phase.

The silicon content of the matrix in zone IV, containing small graphite nodules decreases from 33 to 6 at %. There are normal nodules in zone V while zone IV is a zone in which the graphite morphology transforms from normal spheroid to open nodule, and finally to vermicular and flake graphite as is shown in Fig. 6.

4. Discussion

It was noted that the width of the zones increases with the pouring temperature of the melts and that the dissolution reaction and its associated zones always occur. Sections of these zones were affected by

TABLE I The composition of the RE–Mg alloy

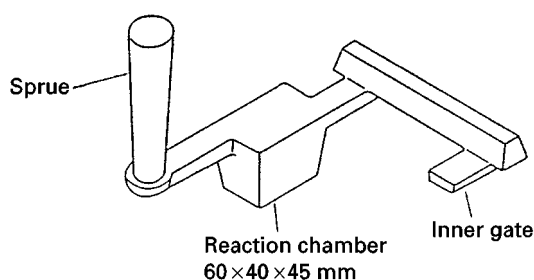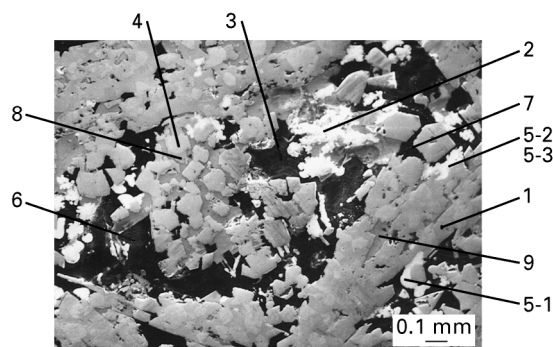| Mg (wt %)	RE (wt %)	Si (wt %)	Fe (wt %)
9	7	45	balance

Figure 1 The gating system.

Figure 2 The secondary electron image of the RE–Mg alloy.

TABLE II The phase composition of the RE–Mg alloy indicated in Fig. 2

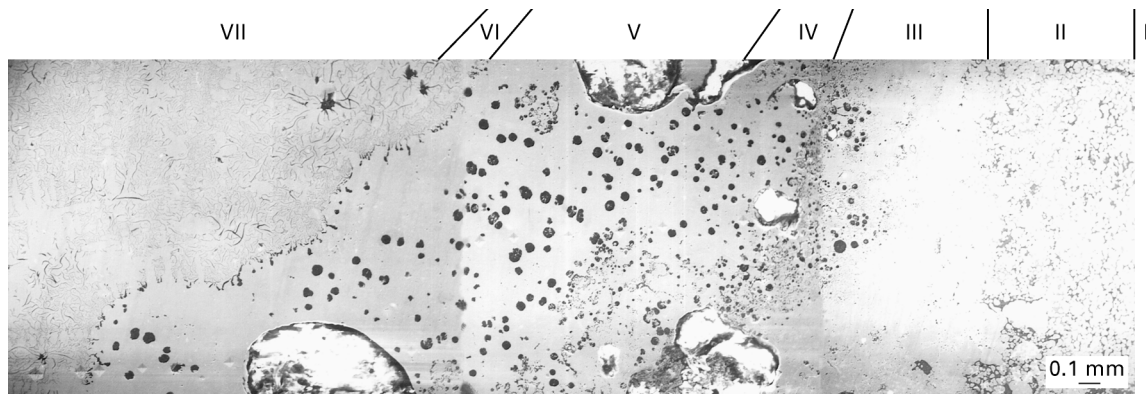| Point	Mg (at %)	Si (at %)	Ca (at %)	Fe (at %)	La (at %)	Ce (at %)	Nd (at %)	Phase
1		74		26				ζ $FeSi_2$
2	28	50	20	2				Mg–Ca–Si
3	42	58		trace				Mg_2Si–Si
4		53		47				ε FeSi
5-1	79	5				16		RE–Si–Ca
5-2	78	4				14	4	RE–Si–Ca
5-3	75	3			4	15	3	RE–Si–Ca
6	47	53						Mg_2Si–Si
8	29	49	18	4				Mg–Ca–Si
9	28	48	20	4				Mg–Ca–Si

Figure 3 The dissolution region of the RE–Mg alloy (secondary electron image).

TABLE III The phases present in the different zones

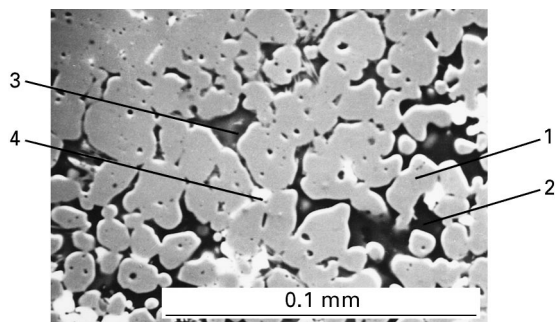| Zone	Si content in matrix (at %)	Phases
I	73 and 50	FeSi$_2$, FeSi, Mg$_2$Si–Si, RE–Ca–Si, Mg–Ca–Si
II	50	FeSi, Mg$_2$Si, SiC, RE–Si
III	33	α, Mg$_2$Si, RE–Ca–Si, small graphite nodules
IV	10	Graphite nodules
V	6	Normal spheroidal graphite
VI	6	Graphite transition zone: spheroidal, vermicular, flake
VII	6	Flake graphite

Figure 5 The boundary between zone II and III.

Figure 4 Zone II of the dissolution region.

Figure 6 The transition graphite zone.

TABLE IV The composition of the points indicated in Figs 4 and 5

Point	Mg (wt %)	Al (wt %)	Si (wt %)	Ca (wt %)	Ce (wt %)	Fe (wt %)	Phase
1			36			64	ε FeSi
2	61		34			5	Mg$_2$Si
3	21		39	13		27	
4	20		37	2	39	2	
5	15	2	44	16	3	20	
6			37			63	ε FeSi

convection and stirring caused by magnesium vapour. However, it is generally consistent to divide the dissolution region into seven zones that constitute the physical model of the dissolution behaviour of the RE–Mg alloy in molten cast iron.
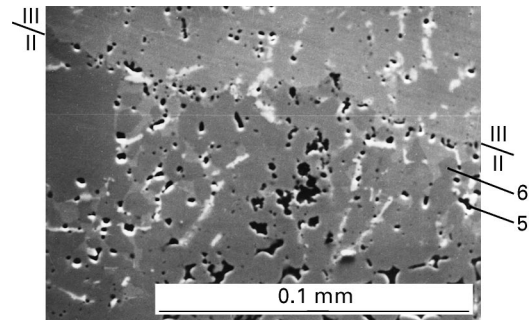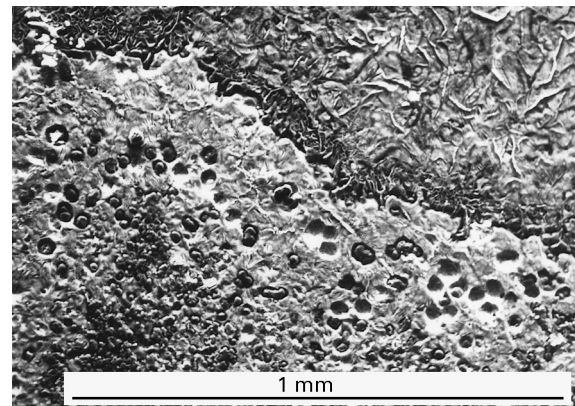
It has been shown that the fusion of the alloy in the reaction chamber is a process in which the alloy melts layer by layer [7, 8]. The process can alternatively be considered as the disintegration of the particles of the alloy. By analysing the dissolution zone structure and by reference to the Fe–Si, Mg–Si and RE–Si phase diagrams, one can deduce that the low melting point phases such as the Mg$_2$Si–Si eutectic, Mg$_2$Si and RE–Ca–Si phase melt first, then the high melting point phases such as the ε phase dissolve later. The ε phase remains in the melt for a period of time when the alloy comes into contact with the molten iron. Therefore the formation of small alloy particles (approximately 10 μm in size) is due to the low melting point phases being the first to melt.

Hurum has isolated the concentration range in the Fe–C–Si diagram in which silicon carbide is formed

[9]. Faivre [10] has investigated the effect of silicon content on the structure of cast iron and confirmed the concentrations necessary to form silicon carbide. When the amount of C and Si reaches a critical value, silicon carbide nucleates and grows. It seems that at a certain Si concentration, SiC decomposes through the diffusion of carbon and self-diffusion of iron. Hurum considered that the disappearance of SiC was a result of the following reaction:

$$Fe + SiC = FeSi + C$$
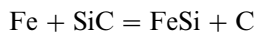
It was observed that many small graphite nodules exist inside the SiC phase, presumably caused by a heavy supersaturation of Si in the surrounding melt following the formation of SiC. The formation of carbides and graphite has been evaluated thermodynamically by Wang and Fredriksson [1] and Fredriksson [2].

Starting from a small nodule, the graphite grows along the a axis $[10\bar{1}0]$ and expands in the c axis direction $[0001]$ like a cylinder or vermicule, afterwards the graphite branches and becomes flake type C, D, and A graphite as shown in Fig. 6. A similar phenomenon was found in directional solidification experiments [11] on a grey iron melt. Since there is no large temperature gradient in the reaction chamber it is considered that varying concentrations of RE and Mg in the solidification front are the main reasons for these growth modes. The transition in the graphite morphology is also due to the existence of Mg and RE in the solidification front. Oxygen and sulfur in a molten iron solution form oxides and sulfides with the Mg and RE. Sadocha and Gruzleske [12] have suggested that the effect of the modifying elements, Mg and RE, is to eliminate S and O on the surface of the graphite and thereby change the interfacial energies between melt and prism planes of graphite, and between melt and basal planes of graphite. The continuous transition in the graphite growth morphologies implies that the concentration of Mg and RE at the solidification front decreases gradually and is insufficient to eliminate the influence of O and S species.

When the Fe–Si alloy is added to the molten cast iron, the carbon activity increases which results in the supersaturation of the melt with carbon, and thus the nucleation and growth of graphite becomes easy. An analysis of the dissolution region reveals that the dissolution of the ε phase is slower than that of the lower melting point phases. When the alloy disintegrates in the melt, the ε phase is distributed on a microscale in the melt. In addition, the SiC dissolves via the diffusion of silicon which reacts with Fe to form the ε phase. These ε phase particles dissolve in the melt and create local areas of high concentration of Si and C, which promotes the nucleation and growth of graphite.

It is expected that the existence of heterogeneous nuclei in the melt decreases the energy of nucleation or the necessary supersaturation of C and Si. In practice, if there is not enough supersaturation of C and Si, the nucleation of graphite will be difficult even if there is large number of inclusions or nucleation sites [2]. Thus it can be seen that the formation of a high local supersaturation is a sufficient and necessary condition for the nucleation of graphite.

The time of inoculation is therefore assumed to be the time between the formation and disappearance of the local supersaturated areas. This is the inoculation mechanism of cast iron.

5. Conclusions
A considerable amount of information about the mechanism of spheroidization in cast iron melts can be obtained by studying the dissolution behaviour of RE–Mg alloys. The dissolution behaviour is observable by investigating the reaction chamber of castings used in the in-mould treatment process. The dissolution zone can be divided into seven zones that reflect the dissolution behaviour of the RE–Mg alloy in the iron melt.

The RE–Mg alloy is composed of several phases and Mg, RE and Ca are present in the form of silicides. The dissolution of the RE–Mg alloy in molten iron is a process in which the low melting point phases such as the Mg_2Si–Si eutectic, Mg_2Si–Si and RE–Ca–Si dissolve first, which causes the disintegration of the alloy and disperses the high melting point phases such as ζ and ε phases into the melt. These phases afterwards dissolve, diffuse and mix so that the melt becomes homogeneous.

Part-way through the dissolution and dispersion phase, the formation of carbides occurs. These carbides are relatively stable in the melt and promote the nucleation and growth of graphite. The decrease of Mg and RE contents makes the morphology of graphite changeable, while inoculation involves the formation of transient supersaturated regions which encourage the nucleation and growth of graphite.

References
1. C. WANG and H. FREDRIKSSON, in Proceedings of the 48th International Foundry Congress, Varna, 1981, p. 16.
2. H. FREDRIKSSON, *Mater. Sci. Engng* **65** (1984) 137.
3. M. REMONDINO, F. PILASTRO, E. NATALE, P. COSTA and G. PERETTI, *AFS Trans.* **82** (1974) 239.
4. C. M. DUNKS, *ibid.* **90** (1982) 551.
5. D. MICHIE, *ibid.* **91** (1983) 855.
6. M. M. SHEA and S. T. HOLTAN, *ibid.* **86** (1978) 13.
7. K. G. DAVIS, R. K. BUHR and J. G. MAGNY, *ibid.* **86** (1978) 379.
8. C. E. DREMANN, *ibid.* **91** (1983) 263.
9. F. HURUM, *ibid.* **60** (1952) 834.
10. R. FAIVRE, *AFS Cast Met. Res. J.* **10** (1974) 15.
11. H. NIESWAAG and A. J. ZUITHOFF, in "Metallurgy of cast iron", edited by B. Lux and I. Minkoff (Georgi Publishing Company, St Saphotin, Switzerland, 1975) p. 327.
12 J. P. SADOCHA and G. A. GRUZLESKE, *ibid.* p. 443.